Eur. Phys. J. B **54**, 315–320 (2006)
DOI: 10.1140/epjb/e2007-00008-8

THE EUROPEAN PHYSICAL JOURNAL B

# Enhanced light emission in Si-nanoclusters arrays

K.I. Mazzitello[1], H.O. Mártin[1], and H.E. Roman[2,a]

[1] Departamento de Física, Facultad de Ciencias Exactas y Naturales, Universidad Nacional de Mar del Plata, Funes 3350, 7600 Mar del Plata, Argentina
[2] Dipartimento di Fisica, Università di Milano-Bicocca, Piazza della Scienza 3, 20126 Milano, Italy

Received 12 June 2006 / Received in final form 18 December 2006
Published online 13 January 2007 – 

**Abstract.** An array of silicon nanoclusters aimed at producing light emission upon injection of electrons and holes from external sources is studied by Monte Carlo simulations. The conditions for obtaining a significant charge accumulation in the emitting nanoclusters are investigated as a function of array geometry and applied electric fields. It is found that if a stationary state, reached for an applied field $F_0$, is suddenly perturbed by a field $F_1 \gg F_0$, a significant increase in electron-hole pairs population can be obtained with respect to the case of a single field of constant intensity $F_1$, leading to enhanced light emission when the conductivity of the array is above $6 \times 10^{-10}$ $[\Omega\ \mathrm{cm}]^{-1}$. The excess population thus created gets fully recombined on the time scale of milliseconds, suggesting a device that can produce enhanced light emission in the range of kilohertz.

**PACS.** 85.60.Jb Light-emitting devices – 05.10.Ln Monte Carlo methods – 73.63.-b Electronic transport in nanoscale materials and structures

## 1 Introduction

A great deal of effort is being concentrated nowadays to the development of silicon-based optoelectronic devices which can emit light efficiently upon injection of charge carriers into the system. Also the question of building a silicon laser remains a central challenge in present technological issues (see e.g. [1–3]). In this context, important progress has been achieved in obtaining the emission of light through the application of an external laser. Recently, optical gain of stimulated infrared light emission has been obtained using a laser source [4].

It is well-known that silicon nanostructures display rather large radiative recombination yields [5–7], suggesting the possibility of employing them as building blocks in appropriately designed device architectures. Two main questions therefore emerge as relevant from a theoretical point of view. On the one hand, it is important to quantify the role that carrier transport plays on the emission process for a generic Si-based device. On the other hand, is it possible to increase the accumulation of charges within the emitting nanoclusters so that the emission of light can be further enhanced?

In this work, we study the conditions for obtaining additional charge accumulation, and therefore enhanced light emission, in a Si nanocluster array as a function of its conductivity. This is important since conductivity limits the current and as a result also the associated light emission power [8]. To this end, we consider the array shown in Figure 1 as the working structure. We assume that electrons and holes are injected from the P and N sources and driven by an applied electric field $F$. The actual value of the conductivity of the hypothetical device shown in Figure 1 is not known, but it is expected to be at least of the order of magnitude of that observed in porous silicon [9].

To study transport along the array, we do not consider the details of the actual contacts between sources and nearby Si nanoclusters (NCs). Rather, carrier hopping across a contact barrier is described as a thermally activated process determined by the difference in optical gaps between the bulk value (1.17 eV within the doped Si-crystals) and the gap of intermediate NCs, assumed to be of 1.25 eV, and between the latter and the smallest NCs of 1.8 eV gaps. The spatial distribution of the gaps create an energy landscape which hinders the motion of carriers towards the center of the array. In addition to this effect, the interaction among charge carriers needs to be taken into account as discussed below (see e.g. [10]).

The paper is organized as follows: Section 2 is devoted to the description of the model of Silicon nanoparticles and the Monte Carlo rules employed in the simulations for the motion of charge carriers. Charge-charge interactions are briefly described. Section 3 contains the results

[a] e-mail: eduardo.roman@mib.infn.it

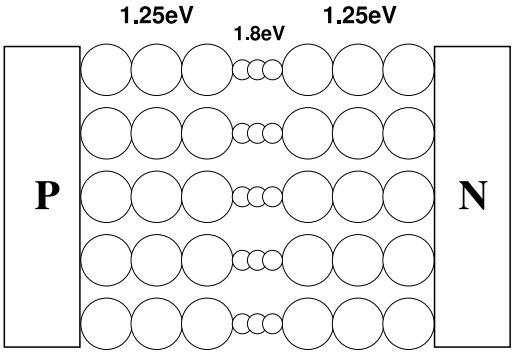


**Fig. 1.** Schematic illustration of an array of Si nanoclusters (open circles) of two different diameters (160 Å and 36 Å), corresponding to optical gaps of 1.25 eV (larger circles) and 1.8 eV (central ones). The large boxes at the borders (denoted by P and N) represent p- and n-type doped silicon crystals with an indirect optical gap of 1.17 eV. In this example, the number of emitting nanoclusters per wire is $L_c = 3$.

for the cases of a single applied field and two alternating external fields. The concluding remarks are summarized in Section 4.

## 2 Silicon nanoclusters model

The larger NCs shown in Figure 1 act as conducting wires for allowing the charge carriers to reach the central ones, the latter having a larger optical gap of about 1.8 eV for which radiative recombinations are most efficient [6]. Transversal transport across such wires is not considered in the present version of the model. In a more realistic picture, the emitting NCs can be imagined to form a granular thin film at the center of the array. The generalization to a three dimensional structure of NCs deposited between the doped silicon plates is straightforward.

Radiative and non-radiative recombination processes are assumed to occur only when both the electron and the hole are present inside the same NC; the former assumed to be exciton-like excitations. The electronic properties of the NCs are described by empirical relations which are functions of the NC radius $R$ (see Refs. [8,11] for details). For instance, for $R \approx 80$ Å, the optical gap becomes $E = 1.25$ eV and the radiative and non radiative recombination times ($\tau_{\rm rad}$ and $\tau_{\rm nrad}$, respectively) obey, $\tau_{\rm rad} \approx 1428\tau_{\rm nrad} = 16$ ms. For the central NCs of radius $R = 18$ Å, $E = 1.8$ eV and both recombination times are of comparable magnitude, i.e. $\tau_{\rm rad} \approx 2\tau_{\rm nrad} = 1.4$ ms, meaning that on average one third of the recombinations will be radiative.

In the numerical simulations, the density of charge carriers inside the doped materials P and N (see Fig. 1) are assumed to be constant. Here, we consider the case of equally doped p- and n-materials having a density of free carriers $\overline{\rho} = 10^{18}$ cm$^{-3}$. The current $I$ is obtained as the mean number of free carriers that enter the array (per wire) per unit of time. The associated current density, $J$, is then estimated as $J = I/d_0^2$ with $d_0 = 200$ Å.

The motion of carriers in the array is described by a hopping process which becomes a biased random walk due to the presence of the applied external field. The charges are assumed to perform jumps between nearest-neighbor NCs governed by a hopping time, $\tau_{\rm hop}$, which is considered as a parameter in our model. For Si-based materials, typical values of $\tau_{\rm hop}$ can vary in the range $10^{-3}$ ms $< \tau_{\rm hop} <$ 1 ms. We will determine the values of $\tau_{\rm hop}$ which are relevant for answering our quest regarding transport behavior of charges and light emission of the prototype array.

The hopping of charges is limited by their mutual interactions [8,10]. Considering an effective one-dimensional model for simplicity, we assume a screened Coulomb interaction between carriers at NCs $i$ and $j$ along the same wire, of the form

$$V_{i,j} = \frac{q_i q_j}{\varepsilon_{\rm eff}|x_i - x_j|}, \qquad \text{for} \quad i \neq j, \tag{1}$$

where $q_i = e(n_{\rm h}(i) - n_{\rm e}(i))$ is the net charge at the $i$th NC (site), $n_{\rm h}(i)$, $n_{\rm e}(i)$ are the corresponding occupation numbers of holes and electrons, $e > 0$ is the unit electric charge and $x_i$ is the position along the wire direction of the $i$th NC. Due to charge neutrality, the net charges inside the P and N materials are zero. Inside a single NC, i.e. for $i = j$, the self-interaction of charges is estimated as (see also [12])

$$V_{i,i} = \frac{q_i^2}{\varepsilon_{\rm eff} R_i}. \tag{2}$$

Additional contributions due to exchange-correlation effects are not explicitely included in the model. They could be considered within the local density approximation as a correction to equation (2) (see e.g. [14]). Here, we take $\varepsilon_{\rm eff} = 2$ which is close to the value of the dielectric constant in porous Si [15].

The Monte Carlo simulations are perfomed according to the Metropolis method at the fixed temperature $T = 300$ K. The values for the recombination times quoted above have been calculated at this particular temperature. For further details on the simulation rules see [8].

## 3 Results

### 3.1 Single external field

In the following, we consider the case of a linear array of nanoclusters (i.e. a single wire in Figure 1), consisting of 200 nanoclusters on each side of the system with optical gap $E = 1.25$ eV, and apply an external field $F_0$ along the nanoclusters wire. Typical charge distributions in their stationary states, obtained for different values of $F_0$, are shown in Figure 2.

As one can see from this figure, charges accumulate around the center of the array but tend to spread along the wire for low intensity fields. For instance, for $F_0 =$ 10 kV/cm charges occupy about 25% of the wire length. Due to recombinations, the occupation number displays a dip at the center where the emitting nanoclusters are

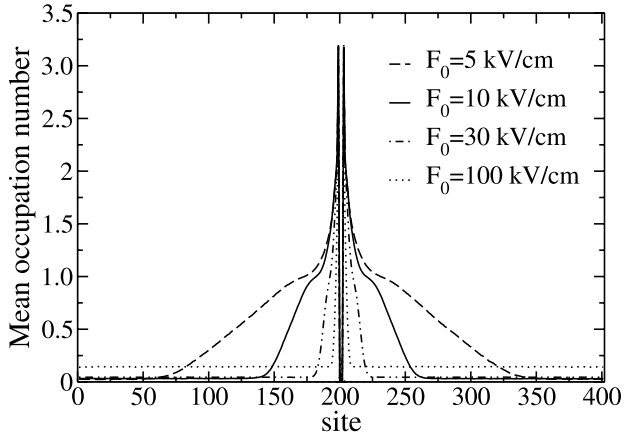


**Fig. 2.** Mean occupation number (per site) of charge carriers (electrons on the right and holes on the left region) in a wire as a function of site position, obtained in the stationary state, for applied external fields: $F_0 = 5$ kV/cm (dashed line), 10 kV/cm (continuous line), 30 kV/cm (dashed dotted line) and 100 kV/cm (dotted line), for the case of $L_c = 3$ emitting nanoclusters per wire and $\tau_{hop} = 5 \times 10^{-2}$ ms.

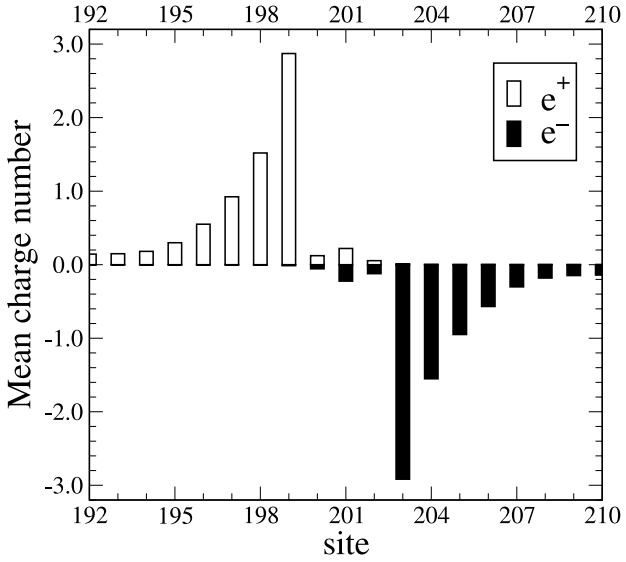


**Fig. 3.** Mean charge number (per site) for electrons and holes as a function of site position, obtained in the stationary state for applied external field $F_0 = 100$ kV/cm, in the case of $L_c = 3$ emitting nanoclusters, for $\tau_{hop} = 5 \times 10^{-2}$ ms.

located. This is more clearly seen in Figure 3 where the charge occupation number is displayed around the center of the array for the case $F_0 = 100$ kV/cm. One can notice the sudden drop in charge occupation in the region where recombinations take place.

The light emission produced by a single external field (as in Figs. 2 and 3) becomes larger the higher is the intensity of the applied field. For instance, for $F_0 = 10$ kV/cm almost no emission is observed, indicating that much larger fields are required to bring a sufficient number of e–h pairs within the emitting NCs.

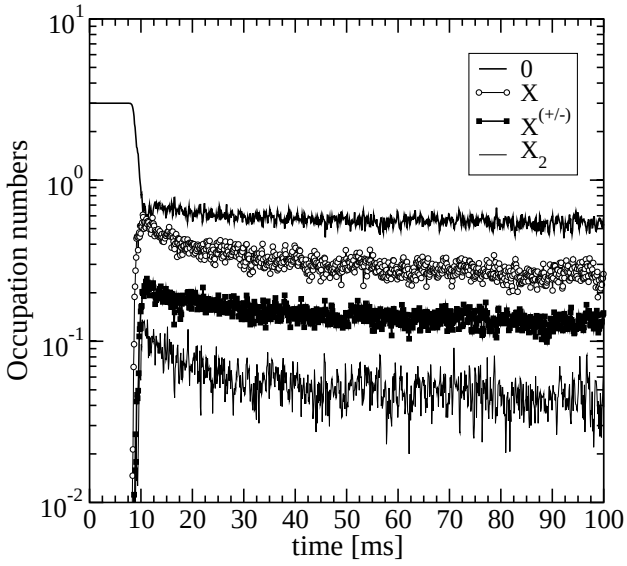


**Fig. 4.** Carrier occupation numbers (inside the $L_c = 3$ central emitting nanoclusters) as a function of time [ms], for: no particles (top continuous line), excitons $X$ (open circles), trions $X^{(+/-)}$ (full squares), and bi-excitons $X_2$ (bottom continuous line), for an external field $F_0 = 500$ kV/cm turned on at $t = 0$. Here, $\tau_{hop} = 5 \times 10^{-2}$ ms. The occupation numbers for single carriers, either an electron or a hole (not shown here for simplicity), become constant and close to 2/3 for times $t > 10$ ms.

In order to better understand the optical behavior of the device in the presence of external fields, it is convenient to consider the temporal behavior of the charge carriers present inside the emitting nanoclusters. Charge carriers can be present in different combinations inside an emitting nanocluster, of which we consider the most important ones. Optically relevant nanoclusters are those in which a single electron-hole pair is present, the latter forming an exciton, denoted as $X$, which upon radiative recombination will produce a photon of 1.8 eV. Other combinations may consist of two electron-hole pairs in a NC (i.e. a biexciton, $X_2$), or one electron (or hole) and one pair (i.e. a trion $X^-$, or $X^+$, respectively). For simplicity, we will assume that in all these cases the radiative recombination energy remains unaltered and equal to 1.8 eV (see e.g. Ref. [16] for a discussion on the dependence of the photon energy on such different configurations).

Illustrative results for the case of a single external field, $F_0 = 500$ kV/cm applied for $t \geq 0$, are shown in Figure 4. The highest occupation numbers correspond to the cases of no-particles, single-particle (e or h) states (not shown in the plot) and excitons, $X$. Note that for this field value the emitting NCs get charged after about 10 ms.

To get further insight into the radiative recombination properties of the array, we consider as a suitable parameter measuring the degree of enhanced charge accumulation in the system the ratio

$$r(t) = \frac{N_1(t)}{N_0(t) + N_1(t)}, \tag{3}$$

where $N_0(t)$ and $N_1(t)$ are the average numbers of emitting NCs that at time $t$ have no particles and one exciton, respectively. Other definitions are possible, however, equation (3) is also interesting for the following reasons.

In a nanocluster, the lowest energy exciton has four substates arising from spin (see e.g. [16]). Two of these exciton substates have angular momentum values equal to $\pm 1$, and are optically active because they can create a photon and decay to the neutral ground state of the undoped and unexcited nanocluster. The other two exciton substates have angular momentum projections equal to $\pm 2$, and are usually denominated dark states since they can not emit a photon when decaying to the neutral ground state. Let us assume that these four substates occur with the same probability in our array. Then, in order to have the same number of optically active nanoclusters as the number of empty ones, one needs to have for each group of six NCs, four of them having one electron-hole pair each and the remaining two being empty. Roughly speaking, such a sort of "inversion of population" will take place when the fraction $r$, equation (3), becomes $r > 4/6 = 2/3$. We expect that the optimum emission of light will occur when $r \geq 2/3$, and in what follows we investigate whether this range of $r$ values can be reached.

### 3.2 Two sequentially applied fields

In what follows, we are interested in the search for enhanced light emission with respect to the single field case based on the use of a suitable combination of external fields. For this purpose, we study next the response to a suddenly increase of the external field from $F_0$ to a value $F_1$ ($F_1 \gg F_0$), at a time that we denote as $t = 0$. The new field pushes further carriers into the emitting zone, thereby initially increasing the number of radiative recombination events. Results for the response of the array to a suddenly increased field $F_1 = 500$ kV/cm are reported in Figure 5, for different initial field values $F_0$ (upper panel) and different numbers of emitting NCs per wire, $L_c$ (lower panel). In these calculations we have used $\tau_{hop} = 5 \times 10^{-2}$ ms.

In the upper panel of the figure, we see that the fraction of charged NCs, $r(t)$ (Eq. (3)), actually overcomes the threshold $r = 2/3$ for moderately low values of $F_0$, within less than 1 ms, and decays to about zero after few ms before raising again to the stationary state value (in this case $r(\infty) \approx 0.4$) corresponding to the new applied field $F_1$. This is an indication that enhanced emission is taking place upon application of a second field. Finally, in the lower panel of Figure 5, we report the effect of $L_c$, indicating that the threshold $r = 2/3$ can be reached for $L_c > 1$ within few ms, depending on $L_c$, displaying a maximum around $L_c = 5$. Again here, the stationary values of $r$ are reached after about 10 ms and depend on $L_c$.

### 3.3 Conductivity and enhanced emission

In order to estimate the conductivity required for making possible such increased accumulation of charge, we consider the case $F_0 = 10$ kV/cm, $F_1 = 500$ kV/cm and $L_c = 3$. The conductivity $\sigma$ is obtained in the stationary state for the applied external field $F_0 = 10$ kV/cm from the relation $\sigma = J/F_0$, where $J$ is the current density (see above). The results are displayed in Figure 6, where the maximum value of $r$, denoted as $r_{max}$, reached in each case is reported as a function of both $\tau_{hop}^{-1}$ and $\sigma$. One can see that $r_{max}$ increases as $\tau_{hop}$ decreases (i.e. $\sigma$ increases). The horizontal line shown in the figure indicates the value $r = 2/3$. This threshold corresponds to a minimum value for $\sigma$ of about $6 \times 10^{-10}$ $[\Omega\ \mathrm{cm}]^{-1}$. The inset in Figure 6 displays the variation of $r$ with time $t$, from which one

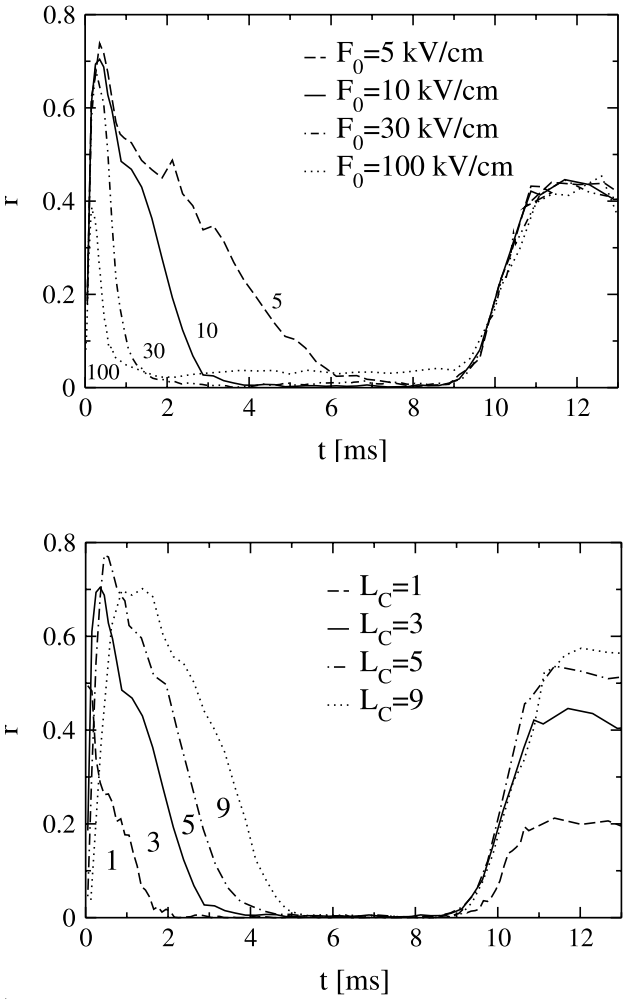


**Fig. 5.** Fraction of charged nanoclusters $r$ (of gap 1.8 eV) as a function of time $t$ [ms], for the case that at $t = 0$ the external electric field is increased, within a time interval $\Delta t = 5 \times 10^{-3}$ ms, from a value $F_0$ (in the stationary state) up to $F_1 = 500$ kV/cm. The new applied field is kept on at its value $F_1$ for $t > 0$. In all cases we have taken $\tau_{hop} = 5 \times 10^{-2}$ ms. *Upper panel*: different initial fields $F_0 = 5$ kV/cm (dashed line), 10 kV/cm (continuous line), 30 kV/cm (dashed dotted line) and 100 kV/cm (dotted line), for the case $L_c = 3$. *Lower panel*: different numbers of emitting nanoclusters per wire (cf. Fig. 1) $L_c = 1$ (dashed line), 3 (continuous line), 5 (dashed dotted line) and 9 (dotted line), for the case $F_0 = 10$ kV/cm.

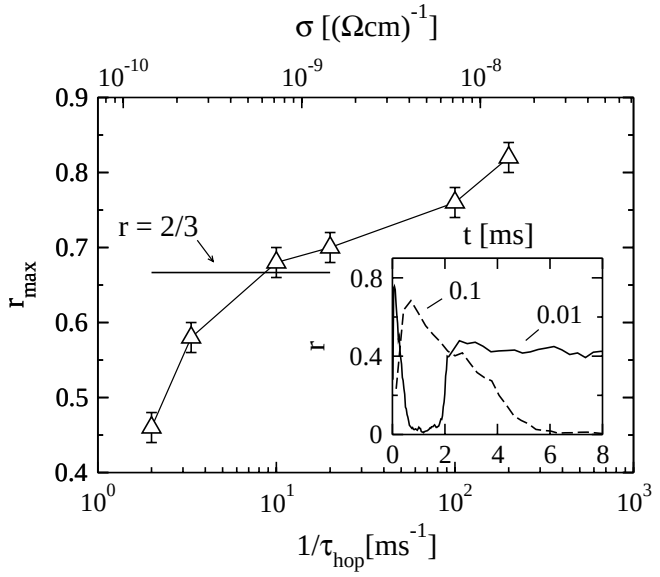


**Fig. 6.** Maximum fraction of charged nanoclusters (of gap 1.8 eV) $r_{\max}$ versus $1/\tau_{\rm hop}$ [$(\rm ms)^{-1}$] (and $r_{\max}$ versus conductivity $\sigma$ [$(\Omega$ cm$)^{-1}$], upper scale), using $F_0 = 10$ kV/cm and $F_1 = 500$ kV/cm, for a NC array with $L_{\rm c} = 3$. The inset shows $r$ versus time $t$ [ms] for two different values of $\tau_{\rm hop}$, $\tau_{\rm hop} = 0.1$ ms (dashed line) and $\tau_{\rm hop} = 10^{-2}$ ms (solid line).

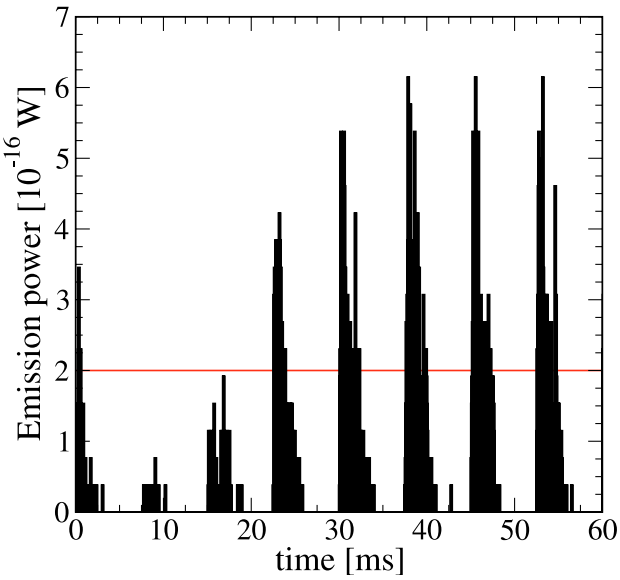


**Fig. 7.** Emission power from the array of nanoclusters (with $L_{\rm c} = 3$) versus time [ms], for the case of alternating external fields $F_0 = 10$ kV/cm, acting during an interval of 5 ms in which the system gets charged, followed by a field $F_1 = 500$ kV/cm acting during a period of 2.5 ms, in which the system gets discharge and emits photons of 1.8 eV. Initially, the system reaches a steady state under the action of $F_0$, and at $t = 0$ the second field $F_1$ is turned on. The horizontal line represents the emission power of the array that would be obtained in the case of a single field of constant intensity 500 kV/cm. Here we used $\tau_{\rm hop} = 5 \times 10^{-2}$ ms.

can estimate the time window over which $r$ remains larger than the threshold, $r > 2/3$. The time widths are found to fall in the range (0.5–1) ms.

Essentially, the useful effects of the second applied field $F_1$ are expected to be exhausted as soon as $r < 2/3$, i.e. after approximately 1 ms $F_1$ can be switched off thus returning to the previous initial conditions determined by the smaller applied field $F_0$. The process can then be repeated periodically afterwards. An illustrative example is displayed in Figure 7, in the case that a field $F_0 = 10$ kV/cm acts during 5 ms, used for charging the system, followed by a field $F_1 = 500$ kV/cm of 2.5 ms duration. The latter induces a bunch of radiative recombinations yielding enhanced light emission, which is higher (by a factor of about 3) than for the case in which a single field of constant intensity 500 kV/cm is applied (the horizontal line in Fig. 7). In this sense, the switching on and off, at intervals of few ms, of a second, higher field, results in enhanced red light emission with respect to the case in which the high field is always on.

## 4 Conclusions

In conclusion, we have studied a simple array of silicon nanoclusters with the aim of estimating the values of the conductivity which can sustain enhanced light emission. The latter can be made possible due to the intrinsic high yields of radiative recombinations in Si NCs (with optical gaps of about 1.8 eV) and on the possibility of dealing with efficient transport behavior of charge carriers through the array.

More specifically, the prediction of the present work is that, for the prototype array shown in Figure 1 there exists a sort of lower bound for the device conductivity, $\sim 6 \times 10^{-10}$ [$\Omega$ cm$]^{-1}$, above which efficient emission of light can be expected. Such enhanced emission can be obtained by using a pulsed external field. There is a crucial difference whether one applies a constant or a pulsed external field. In the former case there is no charge transport for most of the time inside the central emitting nanoclusters even for a large external field of 500 kV/cm (see Fig. 4). Whereas one gets a significant increase in electron-hole pairs population inside the central emitting nanoclustes using a combination of two fields, one of small intensity and applied for few milliseconds to "charge" the system, followed by a much higher one acting for a similar interval of time for producing additional e–h pair recombinations. The fraction $r$ of charged central nanoclusters should be such that $r > 2/3$ to make enhanced light emission efficient. The estimated values of conductivity are expected to be useful for the potential applications of the ideas presented in this work.

Two of us (K.I.M. and H.O.M.) acknowledge financial support from ANPCyT (PICT 2004, No. 03-20075, Argentina) and from the National Council for Scientific and Technical Research (CONICET) of Argentina.

## References


1. L.T. Canham, Nature **408**, 411 (2000)
2. L. Pavesi, J. Phys.: Condensed Matter **15**, 1169 (2003)
3. L. Pavesi, L. dal Negro, C. Mazzoleni, G. Franzó, F. Priolo, Nature **408**, 440 (2000)
4. S.G. Cloutier, P.A. Kossyrev, J. Xu, Nat. Mat. **4**, 887 (2005)
5. M.H. Nayfeh, S. Rao, N. Barry, J. Therrien, G. Belomoin, A. Smith, S. Chaieb, Appl. Phys. Lett. **80**, 121 (2002)
6. G. Ledoux, J. Gong, F. Huisken, O. Guillois, C. Reynaud, Appl. Phys. Lett. **80**, 4834 (2002)
7. A. Fujiwara, K. Yamazaki, Y. Takahashi, Appl. Phys. Lett. **80**, 4567 (2002)
8. K.I. Mazzitello, H.O. Mártin, C.M. Aldao, H.E. Roman, J. Phys. D: Appl. Phys. **37**, 668 (2004)
9. M. Ben-Chorin, F. Möller, F. Koch, W. Schirmacher, M. Eberhard, Phys. Rev. B **51**, 2199 (1995)
10. K.I. Mazzitello, H.O. Mártin, H.E. Roman, Eur. Phys. J. B **46**, 207 (2005)
11. H.E. Roman, L. Pavesi, J. Phys.: Condensed Matter **8**, 5161 (1996)
12. G. Allan, C. Delerue, M. Lannoo, E. Martin, Phys. Rev. B **52**, 11982 (1995)
13. R. Tsu, D. Babić, Appl. Phys. Lett. **64**, 1806 (1994)
14. R.A. Broglia, G. Coló, G. Onida, H.E. Roman, *Solid State Physics of Finite Systems: Metal Clusters, Fullerenes, Atomic Wires* (Springer Verlag, Berlin, 2004)
15. I. Sagnes, A. Halimaoui, G. Vincent, P.A. Badoz, Appl. Phys. Lett. **62**, 1155 (1993)
16. D. Gammon, Al.L. Efros, T.A. Kennedy, M. Rosen, D.S. Katzer, D. Park, S.W. Brown, V.L. Korenev, I.A. Merkulov, Phys. Rev. Lett. **86**, 5176 (2001); D. Gammon, D.G. Steel, Physics Today **55**, 36 (2002)